12

Mass Transfer Related to Heterogeneous Combustion of Solid Carbon in the Forward Stagnation Region - Part 1 - Combustion Rate and Flame Structure

Atsushi Makino
Japan Aerospace Exploration Agency
Japan

1. Introduction

Carbon combustion has been a research subject, relevant to pulverized coal combustion. However, it is not limited to basic research on coal/char combustion, but can benefit various aerospace applications, such as propulsion due to its high energy density and evaluation of protection properties of carbon-carbon composites (C/C-composites) used as high-temperature, structural materials for atmospheric re-entry, gas-turbine blades, scram jet combustors, etc., including ablative carbon heat-shields. Because of practical importance, extensive research has been conducted experimentally, theoretically, and/or numerically, as summarized in several comprehensive reviews (Batchelder, et al., 1953; Gerstein & Coffin, 1956; Walker, et al., 1959; Clark, et al., 1962; Khitrin, 1962; Mulcahy & Smith, 1969; Maahs, 1971; Rosner, 1972; Essenhigh, 1976, 1981; Annamalai & Ryan, 1993; Annamalai, et al., 1994). Nonetheless, because of complexities involved, further studies are required to understand basic nature of the combustion. Some of them also command fundamental interest, because of simultaneous existence of surface and gas-phase reactions, interacting each other.

Generally speaking, processes governing the carbon combustion are as follows: (i) diffusion of oxidizing species to the solid surface, (ii) adsorption of molecules onto active sites on the surface, (iii) formation of products from adsorbed molecules on the surface, (iv) desorption of solid oxides into the gas phase, and (v) migration of gaseous products through the boundary layer into the freestream. Since these steps occur in series, the slowest of them determines the combustion rate and it is usual that steps (ii) and (iv) are extremely fast.

When the surface temperature is low, step (iii) is known to be much slower than steps (i) or (v). The combustion rate, which is also called as the mass burning rate, defined as mass transferred in unit area and time, is then determined by chemical kinetics and therefore the process is kinetically controlled. In this kinetically controlled regime, the combustion rate only depends on the surface temperature, exponentially. Since the process of diffusion, being conducted through the boundary layer, is irrelevant in this regime, the combustion rate is independent of its thickness. Concentrations of oxidizing species at the reacting surface are not too different from those in the freestream. In addition, since solid carbon is more or less porous, in general, combustion proceeds throughout the sample specimen.

On the other hand, when the surface temperature is high, step (iii) is known to be much faster than steps (i) and (v). The combustion rate is then controlled by the diffusion rate of oxidizing species (say, oxygen) to the solid surface, at which their concentrations are negligibly small. In this diffusionally controlled regime, therefore, the combustion rate strongly depends on the boundary layer thickness and weakly on the surface temperature ($\propto T^{0.5\sim1.0}$), with exhibiting surface regression in the course of combustion.

Since oxygen-transfer to the carbon surface can occur via O_2, CO_2, and H_2O, the major surface reactions can be

$$C + O_2 \rightarrow CO_2 , \tag{R1}$$

$$2C + O_2 \rightarrow 2CO , \tag{R2}$$

$$C + CO_2 \rightarrow 2CO , \tag{R3}$$

$$C + H_2O \rightarrow CO + H_2 . \tag{R4}$$

At higher temperatures, say, higher than 1000 K, CO formation is the preferred route and the relative contribution from (R1) can be considered to be negligible (Arthur, 1951). Thus, reaction (R2) will be referred to as the C-O_2 reaction.

Comparing (R2) and (R3), as alternate routes of CO production, the C-O_2 reaction is the preferred route for CO production at low temperatures, in simultaneous presence of O_2 and CO_2. It can be initiated around 600 K and saturated around 1600 K, proceeding infinitely fast, eventually, relative to diffusion. The C-CO_2 reaction of (R3) is the high temperature route, initiated around 1600 K and saturated around 2500 K. It is of particular significance because CO_2 in (R3) can be the product of the gas-phase, water-catalyzed, CO-oxidation,

$$2CO + O_2 \rightarrow 2CO_2 , \tag{R5}$$

referred to as the CO-O_2 reaction. Thus, the C-CO_2 and CO-O_2 reactions can form a loop.

Similarly, the C-H_2O reaction (R4), generating CO and H_2, is also important when the combustion environment consists of an appreciable amount of water. This reaction is also of significance because H_2O is the product of the H_2-oxidation,

$$2H_2 + O_2 \rightarrow 2H_2O , \tag{R6}$$

referred to as the H_2-O_2 reaction, constituting a loop of the C-H_2O and H_2-O_2 reactions.

The present monograph, consisting of two parts, is intended to shed more light on the carbon combustion, with putting a focus on its heat and mass transfer from the surface. It is, therefore, not intended as a collection of engineering data or an exhaustive review of all the pertinent published work. Rather, it has an intention to represent the carbon combustion by use of some of the basic characteristics of the chemically reacting boundary layers, under recognition that flow configurations are indispensable for proper evaluation of the heat and mass transfer, especially for the situation in which the gas-phase reaction can intimately affect overall combustion response through its coupling to the surface reactions.

Among various flow configurations, it has been reported that the stagnation-flow configuration has various advantages, because it provides a well-defined, one-dimensional flow, characterized by a single parameter, called the stagnation velocity gradient. It has even been said that mathematical analyses, experimental data acquisition, and physical

interpretations have been facilitated by its introduction. Therefore, we will confine ourselves to studying carbon combustion in the axisymmetric stagnation flow over a flat plate and/or that in the two-dimensional stagnation flow over a cylinder. From the practical point of view, we can say that it simulates the situations of ablative carbon heat-shields and/or strongly convective burning in the forward stagnation region of a particle.

In this Part 1, formulation of the governing equations is first presented in Section 2, based on theories on the chemically reacting boundary layer in the forward stagnation field. Chemical reactions considered include the surface C-O_2 and C-CO_2 reactions and the gas-phase CO-O_2 reaction, for a while. Generalized species-enthalpy coupling functions are then derived without assuming any limit or near-limit behaviors, which not only enable us to minimize the extent of numerical efforts needed for generalized treatment, but also provide useful insight into the conserved scalars in the carbon combustion. In Section 3, it is shown that straightforward derivation of the combustion response can be allowed in the limiting situations, such as those for the Frozen, Flame-detached, and Flame-attached modes.

In Section 4, after presenting profiles of gas-phase temperature, measured over the burning carbon, a further analytical study is made about the ignition phenomenon, related to finite-rate kinetics, by use of the asymptotic expansion method to obtain a critical condition. Appropriateness of this criterion is further examined by comparing temperature distributions in the gas phase and/or surface temperatures at which the CO-flame can appear. After having constructed these theories, evaluations of kinetic parameters for the surface and gas-phase reactions are conducted in Section 5, in order to make experimental comparisons, further.

Concluding remarks for Part 1 are made in Section 6, with references cited and nomenclature tables. Note that the useful information obtained is further to be used in Part 2, to explore carbon combustion at high velocity gradients and/or in the High-Temperature Air Combustion, with taking account of effects of water-vapor in the oxidizing-gas.

2. Formulation

Among previous studies (Tsuji & Matsui, 1976; Adomeit, et al., 1976; Adomeit, et al., 1985; Henriksen, et al., 1988; Matsui & Tsuji, 1987), it may be noted that Adomeit's group has made a great contribution by clarifying water-catalyzed CO-O_2 reaction (Adomeit, et al., 1976), conducting experimental comparisons (Adomeit, et al., 1985), and investigating ignition/extinction behavior (Henriksen, et al., 1988). Here, an extension of the worthwhile contributions is made along the following directions. First, simultaneous presence of the surface C-O_2 and C-CO_2 reactions and the gas-phase CO-O_2 reaction are included, so as to allow studies of surface reactions over an extended range of its temperatures, as well as examining their coupling with the gas-phase reaction. Second, a set of generalized coupling functions (Makino & Law, 1986) are conformed to the present flow configuration, in order to facilitate mathematical development and/or physical interpretation of the results. Third, an attempt is made to identify effects of thermophysical properties, as well as other kinetic and system parameters involved.

2.1 Model definition

The present model simulates the isobaric carbon combustion of constant surface temperature T_s in the stagnation flow of temperature T_∞, oxygen mass-fraction $Y_{O,\infty}$, and carbon dioxide mass-fraction $Y_{P,\infty}$, in a general manner (Makino, 1990). The major reactions

considered here are the surface C-O_2 and C-CO_2 reactions and the gas-phase CO-O_2 reaction. The surface C+O_2→CO_2 reaction is excluded (Arthur, 1951) because our concern is the combustion at temperatures above 1000 K. Crucial assumptions introduced are conventional, constant property assumptions with unity Lewis number, constant average molecular weight, constant value of the product of density ρ and viscosity μ, one-step overall irreversible gas-phase reaction, and first-order surface reactions. Surface characteristics, such as porosity and internal surface area, are grouped into the frequency factors for the surface reactions.

2.2 Governing equations

The steady-state two-dimensional and/or axisymmetric boundary-layer flows with chemical reactions are governed as follows (Chung, 1965; Law, 1978):

Continuity:
$$\frac{\partial\left(\rho u R^j\right)}{\partial x}+\frac{\partial\left(\rho v R^j\right)}{\partial y}=0\,, \tag{1}$$

Momentum:
$$\rho u\frac{\partial u}{\partial x}+\rho v\frac{\partial u}{\partial y}-\frac{\partial}{\partial y}\left(\mu\frac{\partial u}{\partial y}\right)=\rho_\infty u_\infty\left(\frac{\partial u}{\partial x}\right)_\infty\,, \tag{2}$$

Species:
$$\rho u\frac{\partial Y_i}{\partial x}+\rho v\frac{\partial Y_i}{\partial y}-\frac{\partial}{\partial y}\left(\rho D\frac{\partial Y_i}{\partial y}\right)=-w_i \quad (i = \mathrm{F, O}), \tag{3}$$

$$\rho u\frac{\partial Y_\mathrm{P}}{\partial x}+\rho v\frac{\partial Y_\mathrm{P}}{\partial y}-\frac{\partial}{\partial y}\left(\rho D\frac{\partial Y_\mathrm{P}}{\partial y}\right)=w_\mathrm{P}\,, \tag{4}$$

$$\rho u\frac{\partial Y_\mathrm{N}}{\partial x}+\rho v\frac{\partial Y_\mathrm{N}}{\partial y}-\frac{\partial}{\partial y}\left(\rho D\frac{\partial Y_\mathrm{N}}{\partial y}\right)=0\,, \tag{5}$$

Energy:
$$\rho u\frac{\partial\left(c_\mathrm{p}T\right)}{\partial x}+\rho v\frac{\partial\left(c_\mathrm{p}T\right)}{\partial y}-\frac{\partial}{\partial y}\left(\lambda\frac{\partial T}{\partial y}\right)=qw_\mathrm{F}\,, \tag{6}$$

where T is the temperature, c_p the specific heat, q the heat of combustion per unit mass of CO, Y the mass fraction, u the velocity in the tangential direction x, v the velocity in the normal direction y, and the subscripts C, F, O, P, N, g, s, and ∞, respectively, designate carbon, carbon monoxide, oxygen, carbon dioxide, nitrogen, the gas phase, the surface, and the freestream.

In these derivations, use has been made of assumptions that the pressure and viscous heating are negligible in Eq. (6), that a single binary diffusion coefficient D exists for all species pairs, that c_p is constant, and that the CO-O_2 reaction can be represented by a one-step, overall, irreversible reaction with a reaction rate

$$w_\mathrm{F}=\left(\nu_i W_i\right)B_\mathrm{g}\left(\frac{\rho Y_\mathrm{F}}{W_\mathrm{F}}\right)^{\nu_\mathrm{F}}\left(\frac{\rho Y_\mathrm{O}}{W_\mathrm{O}}\right)^{\nu_\mathrm{O}}\exp\left(-\frac{E_\mathrm{g}}{R^o T}\right), \tag{7}$$

where B is the frequency factor, E the activation energy, R^0 the universal gas constant, ν the stoichiometric coefficient, and W the molecular weight. We should also note that R^j in Eq. (1) describes the curvature of the surface such that j = 0 and 1 designate two-dimensional and axisymmetric flows, respectively, and the velocity components u_∞ and v_∞ of the frictionless flow outside the boundary layer are given by use of the velocity gradient a as

$$u_\infty = ax\,, \qquad v_\infty = -(j+1)ay \tag{8}$$

2.3 Boundary conditions

The boundary conditions for the continuity and the momentum equations are the well-known ones, expressed as

$$\begin{aligned} &\text{at } y=0: && u = 0\,, && v = v_s\,, \\ &\text{as } y\to\infty: && && v = v_\infty\,. \end{aligned} \tag{9}$$

For the species conservation equations, we have in the freestream as

$$(Y_\mathrm{F})_\infty = 0, \quad (Y_i)_\infty = Y_{i,\infty} \quad (i = \mathrm{O, P, N}). \tag{10}$$

At the carbon surface, components transported from gas to solid by diffusion, transported away from the interface by convection, and produced/consumed by surface reactions are to be considered. Then, we have

$$(\rho v Y_\mathrm{F})_\mathrm{s} - \left(\rho D \frac{\partial Y_\mathrm{F}}{\partial y}\right)_\mathrm{s} = 2W_\mathrm{F}\left(\frac{\rho Y_\mathrm{O}}{W_\mathrm{O}}\right)_\mathrm{s} B_{\mathrm{s,O}} \exp\left(-\frac{Ta_{\mathrm{s,O}}}{T_\mathrm{s}}\right) + 2W_\mathrm{F}\left(\frac{\rho Y_\mathrm{P}}{W_\mathrm{P}}\right)_\mathrm{s} B_{\mathrm{s,P}} \exp\left(-\frac{Ta_{\mathrm{s,P}}}{T_\mathrm{s}}\right), \tag{11}$$

$$(\rho v Y_\mathrm{O})_\mathrm{s} - \left(\rho D \frac{\partial Y_\mathrm{O}}{\partial y}\right)_\mathrm{s} = -W_\mathrm{O}\left(\frac{\rho Y_\mathrm{O}}{W_\mathrm{O}}\right)_\mathrm{s} B_{\mathrm{s,O}} \exp\left(-\frac{Ta_{\mathrm{s,O}}}{T_\mathrm{s}}\right), \tag{12}$$

$$(\rho v Y_\mathrm{P})_\mathrm{s} - \left(\rho D \frac{\partial Y_\mathrm{P}}{\partial y}\right)_\mathrm{s} = -W_\mathrm{P}\left(\frac{\rho Y_\mathrm{P}}{W_\mathrm{P}}\right)_\mathrm{s} B_{\mathrm{s,P}} \exp\left(-\frac{Ta_{\mathrm{s,P}}}{T_\mathrm{s}}\right), \tag{13}$$

$$(\rho v Y_\mathrm{N})_\mathrm{s} - \left(\rho D \frac{\partial Y_\mathrm{N}}{\partial y}\right)_\mathrm{s} = 0\,. \tag{14}$$

2.4 Conservation equations with nondimensional variables and parameters

In boundary layer variables, the conservation equations for momentum, species i, and energy are, respectively,

$$\frac{d^3 f}{d\eta^3} + f\frac{d^2 f}{d\eta^2} + \frac{1}{2^j}\left\{\frac{\rho_\infty}{\rho} - \left(\frac{df}{d\eta}\right)^2\right\} = 0\,, \tag{15}$$

$$\mathcal{L}\left(\tilde{Y}_\mathrm{F} + \tilde{Y}_\mathrm{P}\right) = \mathcal{L}\left(\tilde{Y}_\mathrm{O} + \tilde{Y}_\mathrm{P}\right) = \mathcal{L}\left(\tilde{Y}_\mathrm{P} - \tilde{T}\right) = \mathcal{L}\left(\tilde{Y}_\mathrm{N}\right) = 0\,, \tag{16}$$

$$\mathcal{L}\left(\tilde{T}\right) = -Da_{\mathrm{g}}\omega_{\mathrm{g}}\,, \tag{17}$$

where the convective-diffusive operator is defined as

$$\mathcal{L} = \frac{d^2}{d\eta^2} + f\frac{d}{d\eta}\,. \tag{18}$$

The present Damköhler number for the gas-phase CO-O_2 reaction is given by

$$Da_{\mathrm{g}} = \left(\frac{B_{\mathrm{g}}}{2^j a}\right)\left(\frac{\rho_\infty}{\nu_{\mathrm{P}} W_{\mathrm{P}}}\right)^{\nu_{\mathrm{F}}+\nu_{\mathrm{O}}-1}(\nu_{\mathrm{F}})^{\nu_{\mathrm{F}}}(\nu_{\mathrm{O}})^{\nu_{\mathrm{O}}}\,, \tag{19}$$

with the nondimensional reaction rate

$$\omega_{\mathrm{g}} = \left(\frac{\tilde{T}_\infty}{\tilde{T}}\right)^{\nu_{\mathrm{F}}+\nu_{\mathrm{O}}-1}\left(\tilde{Y}_{\mathrm{F}}\right)^{\nu_{\mathrm{F}}}\left(\tilde{Y}_{\mathrm{O}}\right)^{\nu_{\mathrm{O}}}\exp\left(-\frac{\tilde{T}a_{\mathrm{g}}}{\tilde{T}}\right). \tag{20}$$

In the above, the conventional boundary-layer variables s and η, related to the physical coordinates x and y, are

$$s = \int_0^x \rho_\infty(x)\,\mu_\infty(x)\,u_\infty(x)\,R^{2j}\,dx\,, \tag{21}$$

$$\eta = \frac{u_\infty(x)R^j}{\sqrt{2s}}\int_0^y \rho(x,y)\,dy\,. \tag{22}$$

The nondimensional streamfunction $f(s,\eta)$ is related to the streamfunction $\psi(x, y)$ through

$$f(s,\eta) = \frac{\psi(x,y)}{\sqrt{2s}}\,, \tag{23}$$

where $\psi(x, y)$ is defined by

$$\rho u R^j = \frac{\partial\psi}{\partial y}, \qquad \rho v R^j = -\frac{\partial\psi}{\partial x}\,, \tag{24}$$

such that the continuity equation is automatically satisfied. Variables and parameters are:

$$\tilde{T} = \frac{T}{q/(c_p\alpha_{\mathrm{F}})}, \qquad \tilde{T}a = \frac{E/R^o}{q/(c_p\alpha_{\mathrm{F}})}, \qquad \alpha_{\mathrm{F}} = \frac{\nu_{\mathrm{P}}W_{\mathrm{P}}}{\nu_{\mathrm{F}}W_{\mathrm{F}}},$$

$$\tilde{Y}_{\mathrm{F}} = \frac{\nu_{\mathrm{P}}W_{\mathrm{P}}}{\nu_{\mathrm{F}}W_{\mathrm{F}}}Y_{\mathrm{F}}, \qquad \tilde{Y}_{\mathrm{O}} = \frac{\nu_{\mathrm{P}}W_{\mathrm{P}}}{\nu_{\mathrm{O}}W_{\mathrm{O}}}Y_{\mathrm{O}}, \qquad \tilde{Y}_{\mathrm{N}} = Y_{\mathrm{N}}, \qquad \delta = \frac{W_{\mathrm{P}}}{W_{\mathrm{C}}}\,.$$

Here, use has been made of an additional assumption that the Prandtl and Schmidt numbers are unity. Since we adopt the ideal-gas equation of state under an assumption of constant, average molecular weight across the boundary layer, the term (ρ_∞/ρ) in Eq. (15) can be

replaced by (T/T_∞). As for the constant ρμ assumption, while enabling considerable simplification, it introduces 50%-70% errors in the transport properties of the gas in the present temperature range. However, these errors are acceptable for far greater errors in the chemical reaction rates. Furthermore, they are anticipated to be reduced due to the change of composition by the chemical reactions.
The boundary conditions for Eq. (15) are

$$f(0)=f_s, \qquad \left(\frac{df}{d\eta}\right)_s=0, \qquad \left(\frac{df}{d\eta}\right)_\infty=1, \tag{25}$$

whereas those for Eqs. (16) and (17) are

$$\begin{aligned} &\text{at } \eta=0: \quad \tilde{T}=\tilde{T}_s, \qquad \tilde{Y}_i=\left(\tilde{Y}_i\right)_s \qquad (i\text{=F, O, P, N}), \\ &\text{as } \eta\to\infty: \ \tilde{T}=\tilde{T}_\infty, \qquad \tilde{Y}_F=0, \qquad \tilde{Y}_i=\left(\tilde{Y}_i\right)_\infty \qquad (i\text{= O, P, N}), \end{aligned} \tag{26}$$

which are to be supplemented by the following conservation relations at the surface:

$$-\left(\frac{d\tilde{Y}_F}{d\eta}\right)_s+\left(-f_s\right)\tilde{Y}_{F,s}=\delta\left(-f_{s,O}\right)+2\delta\left(-f_{s,P}\right)=\delta\left(-f_s\right)+\delta\left(-f_{s,P}\right), \tag{27}$$

$$-\left(\frac{d\tilde{Y}_O}{d\eta}\right)_s+\left(-f_s\right)\tilde{Y}_{O,s}=-\delta\left(-f_{s,O}\right)=-\delta\left(-f_s\right)+\delta\left(-f_{s,P}\right), \tag{28}$$

$$-\left(\frac{d\tilde{Y}_P}{d\eta}\right)_s+\left(-f_s\right)\tilde{Y}_{P,s}=-\delta\left(-f_{s,P}\right), \tag{29}$$

$$-\left(\frac{d\tilde{Y}_N}{d\eta}\right)_s+\left(-f_s\right)\tilde{Y}_{N,s}=0, \tag{30}$$

where

$$\delta\left(-f_s\right)=\delta\left(-f_{s,O}\right)+\delta\left(-f_{s,P}\right)=A_{s,O}\tilde{Y}_{O,s}+A_{s,P}\tilde{Y}_{P,s}\ ; \tag{31}$$

$$A_{s,O}\equiv Da_{s,O}\left(\frac{\tilde{T}_\infty}{\tilde{T}_s}\right)\exp\left(-\frac{\tilde{T}a_{s,O}}{\tilde{T}_s}\right); \quad Da_{s,O}\equiv\frac{B_{s,O}}{\sqrt{2^j a\left(\mu_\infty/\rho_\infty\right)}},$$

$$A_{s,P}\equiv Da_{s,P}\left(\frac{\tilde{T}_\infty}{\tilde{T}_s}\right)\exp\left(-\frac{\tilde{T}a_{s,P}}{\tilde{T}_s}\right); \quad Da_{s,P}\equiv\frac{B_{s,P}}{\sqrt{2^j a\left(\mu_\infty/\rho_\infty\right)}},$$

and $Da_{s,O}$ and $Da_{s,P}$ are the present surface Damköhler numbers, based only on the frequency factors for the C-O_2 and C-CO_2 reactions, respectively. Here, these heterogeneous

reactions are assumed to be first order, for simplicity and analytical convenience.[1] As for the kinetic expressions for non-permeable solid carbon, effects of porosity and/or internal surface area are considered to be incorporated, since surface reactions are generally controlled by combinations of chemical kinetics and pore diffusions.
For self-similar flows, the normal velocity v_s at the surface is expressible in terms of $(-f_s)$ by

$$(\rho v)_s = (-f_s)\sqrt{2^j a\, \rho_\infty \mu_\infty} \ . \tag{32}$$

Reminding the fact that the mass burning rate of solid carbon is given by $\dot{m} = (\rho v)_s$, which is equivalent to the definition of the combustion rate [kg/(m²·s)], then $(-f_s)$ can be identified as the nondimensional combustion rate. Note also that the surface reactions are less sensitive to velocity gradient variations than the gas-phase reaction because $Da_s \sim a^{-1/2}$ while $Da_g \sim a^{-1}$.

2.5 Coupling functions

With the boundary conditions for species, cast in the specific forms of Eqs. (27) to (29), the coupling functions for the present system are given by

$$\tilde{Y}_F + \tilde{Y}_P = \frac{\left(\tilde{Y}_{P,\infty} + \delta\beta\right) + \left(\tilde{Y}_{P,\infty} - \delta\right)\beta\xi}{1+\beta}, \tag{33}$$

$$\tilde{Y}_O + \tilde{Y}_P = \frac{\left(\tilde{Y}_{O,\infty} + \tilde{Y}_{P,\infty} - \delta\beta\right) + \left(\tilde{Y}_{O,\infty} + \tilde{Y}_{P,\infty} + \delta\right)\beta\xi}{1+\beta}, \tag{34}$$

$$\tilde{Y}_O + \tilde{T} = \tilde{Y}_{O,s} + \tilde{T}_s + \left(\tilde{Y}_{O,\infty} - \tilde{Y}_{O,s} + \tilde{T}_\infty - \tilde{T}_s\right)\xi; \qquad \tilde{Y}_{O,s} = \frac{\tilde{Y}_{O,\infty} + \tilde{T}_\infty - \tilde{T}_s - \gamma}{1+\beta+A_{s,O}\left[\beta/(-f_s)\right]}, \tag{35}$$

$$\tilde{Y}_P - \tilde{T} = \tilde{Y}_{P,s} - \tilde{T}_s + \left(\tilde{Y}_{P,\infty} - \tilde{Y}_{P,s} - \tilde{T}_\infty + \tilde{T}_s\right)\xi; \qquad \tilde{Y}_{P,s} = \frac{\tilde{Y}_{P,\infty} - \tilde{T}_\infty + \tilde{T}_s + \gamma}{1+\beta+A_{s,P}\left[\beta/(-f_s)\right]}, \tag{36}$$

$$\tilde{Y}_N = \tilde{Y}_{N,\infty}\frac{1+\beta\,\xi}{1+\beta}, \tag{37}$$

where

$$\xi = \frac{\int_0^\eta \exp\left(-\int_0^\eta f\,d\eta\right)d\eta}{\int_0^\infty \exp\left(-\int_0^\eta f\,d\eta\right)d\eta}, \tag{38}$$

$$\gamma = \frac{\left(\tilde{T}'\right)_s}{(\xi')_s}, \qquad \beta = \frac{(-f_s)}{(\xi')_s}, \qquad (\xi')_s = \frac{1}{\int_0^\infty \exp\left(-\int_0^\eta f\,d\eta\right)d\eta}, \tag{39}$$

[1]The surface C-O_2 reaction of half-order is also applicable (Makino, 1990).

and a prime indicates $d/d\eta$. Using the new independent variable ξ, the energy conservation Eq. (17) becomes

$$\left(\frac{d^2\tilde{T}}{d\xi^2}\right) = -\frac{Da_g \omega_g}{(d\xi/d\eta)^2} \,. \tag{40}$$

Therefore, the equations to be solved are Eqs. (15) and (40), subject to the boundary conditions in Eq. (25) and

$$\left(\tilde{T}\right)_{\xi=0} = \tilde{T}_s, \qquad \left(\tilde{T}\right)_{\xi=1} = \tilde{T}_\infty \,, \tag{41}$$

by use of $(-f_s)$ given by Eq. (31) and the coupling functions in Eqs. (33) to (36). Key parameters in solving those are Da_g, $Da_{s,O}$, $Da_{s,P}$, and $(-f_s)$.

2.6 Transfer number and combustion rate

The influence of finite rate gas-phase kinetics is studied here. The global rate equation used has the same form as that of Howard, et al. (1973), in which the activation energy and the frequency factor are reported to be E_g=113 kJ/mol and B_g=1.3×10^8 [(mol/m^3)·s]$^{-1}$, respectively. The combustion response is quite similar to that of particle combustion (Makino & Law, 1986), as shown in Fig. 1(a) (Makino, 1990). The parameter β, indispensable in obtaining the combustion rate, is bounded by limiting solutions to be mentioned, presenting that the gas-phase CO-O_2 reaction reduces the surface C-O_2 reaction by consuming O_2, while at the same time initiating the surface C-CO_2 reaction by supplying CO_2, and that with increasing surface temperature the combustion rate can first increase, then decrease, and increase again as a result of the close coupling between the three reactions. In addition, the combustion process depends critically on whether the gas-phase CO-O_2 reaction is activated. If it is not, the oxygen in the ambience can readily reach the surface to participate in the C-O_2 reaction. Activation of the surface C-CO_2 reaction depends on whether the environment contains any CO_2. However, if the gas-phase CO-O_2 reaction is activated, the existence of CO-flame in the gas phase cuts off most of the oxygen supplied to the surface such that the surface C-O_2 reaction is suppressed. At the same time, the CO_2 generated at the flame activates the surface C-CO_2 reaction.

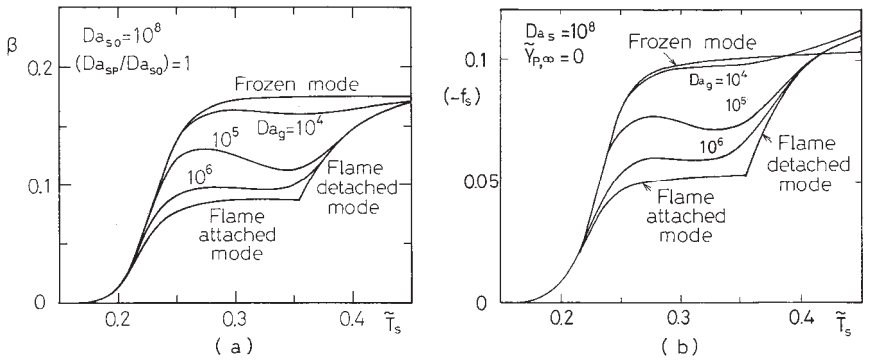

Fig. 1. Combustion behavior as a function of the surface temperature with the gas-phase Damköhler number taken as a parameter; $Da_{s,O}$= $Da_{s,P}$=10^8 and $Y_{P,\infty}$=0 (Makino, 1990). (a) Transfer number. (b) Nondimensional combustion rate.

It may informative to note that the parameter β, defined as $(-f_s)/(\xi')_s$ in the formulation, coincides with the conventional transfer number (Spalding, 1951), which has been shown by considering elemental carbon, $(W_C/W_F)Y_F+(W_C/W_P)Y_P$, taken as the transferred substance, and by evaluating driving force and resistance, determined by the transfer rate in the gas phase and the ejection rate at the surface, respectively (Makino, 1992; Makino, et al., 1998). That is,

$$\frac{\left(\frac{W_C Y_F}{W_F}+\frac{W_C Y_P}{W_P}\right)_s-\left(\frac{W_C Y_F}{W_F}+\frac{W_C Y_P}{W_P}\right)_\infty}{1-\left(\frac{W_C Y_F}{W_F}+\frac{W_C Y_P}{W_P}\right)_s}=\frac{\left(\tilde{Y}_F+\tilde{Y}_P\right)_s-\left(\tilde{Y}_F+\tilde{Y}_P\right)_\infty}{\delta-\left(\tilde{Y}_F+\tilde{Y}_P\right)_s}\equiv\beta\,. \tag{42}$$

Figure 1(b) shows the combustion rate in the same conditions. At high surface temperatures, because of the existence of high-temperature reaction zone in the gas phase, the combustion rate is enhanced. In this context, the transfer number, less temperature-sensitive than the combustion rate, as shown in Figs. 1(a) and 1(b), is preferable for theoretical considerations.

3. Combustion behavior in the limiting cases

Here we discuss analytical solutions for some limiting cases of the gas-phase reaction, since several limiting solutions regarding the intensity of the gas-phase CO-O_2 reaction can readily be identified from the coupling functions. In addition, important characteristics indispensable for fundamental understanding is obtainable.

3.1 Frozen mode

When the gas-phase CO-O_2 reaction is completely frozen, the solution of the energy conservation Eq. (17) readily yields

$$\tilde{T}=\tilde{T}_s+\gamma\,\xi\,;\quad \gamma=\tilde{T}_\infty-\tilde{T}_s\,. \tag{43}$$

Evaluating Eqs. (35) and (36) at ξ=0 for obtaining surface concentrations of O_2 and CO_2, and substituting them into Eq. (31), we obtain an implicit expression for the combustion rate $(-f_s)$

$$\delta(-f_s)=A_{s,O}\frac{\tilde{Y}_{O,\infty}}{1+\beta+A_{s,O}\left[\beta/(-f_s)\right]}+A_{s,P}\frac{\tilde{Y}_{P,\infty}}{1+\beta+A_{s,P}\left[\beta/(-f_s)\right]}\,, \tag{44}$$

which is to be solved numerically from Eq. (15), because of the density coupling. The combustion rate in the diffusion controlled regime becomes the highest with satisfying the following condition.

$$\beta_{max}=\frac{\tilde{Y}_{O,\infty}+\tilde{Y}_{P,\infty}}{\delta} \tag{45}$$

3.2 Flame-detached mode

When the gas-phase CO-O_2 reaction occurs infinitely fast, two flame-sheet burning modes are possible. One involves a detached flame-sheet, situated away from the surface, and

the other an attached flame-sheet, situated on the surface. The Flame-detached mode is defined by

$$\widetilde{Y}_{\mathrm{O}}\left(0 \le \xi \le \xi_f\right) = \widetilde{Y}_{\mathrm{F}}\left(\xi_f \le \xi \le \infty\right) = 0\,. \tag{46}$$

By using the coupling functions in Eqs. (33) to (36), it can be shown that

$$\delta\left(-f_{\mathrm{s}}\right) = A_{\mathrm{s,P}}\frac{\widetilde{Y}_{\mathrm{O},\infty} + \widetilde{Y}_{\mathrm{P},\infty} - \delta\beta}{1+\beta} \tag{47}$$

$$\widetilde{T}_f = \widetilde{T}_{\mathrm{s}} + \left(\widetilde{Y}_{\mathrm{O},\infty} + \widetilde{T}_\infty - \widetilde{T}_{\mathrm{s}}\right)\xi_f\,; \qquad \xi_f = \frac{2\delta\beta - \widetilde{Y}_{\mathrm{O},\infty}}{\left(2\delta + \widetilde{Y}_{\mathrm{O},\infty}\right)\beta}, \tag{48}$$

Once ($-f_{\mathrm{s}}$) is determined from Eqs. (47) and (15), ξ_f can readily be evaluated, yielding the temperature distribution as

$$0 \le \xi \le \xi_f: \quad \widetilde{T} = \widetilde{T}_{\mathrm{s}} + \left(\widetilde{Y}_{\mathrm{O},\infty} + \widetilde{T}_\infty - \widetilde{T}_{\mathrm{s}}\right)\xi\,, \tag{49}$$

$$\xi_f \le \xi \le \infty: \quad \widetilde{T} = \widetilde{T}_\infty - \left\{\widetilde{T}_\infty - \widetilde{T}_{\mathrm{s}} + \left(\frac{\widetilde{Y}_{\mathrm{O},\infty} - 2\delta\beta}{1+\beta}\right)\left(1-\xi\right)\right\}. \tag{50}$$

In addition, the infinitely large Da_{g} yields the following important characteristics, as reported by Tsuji & Matsui (1976).

1. The quantities Y_{F} and Y_{O} in the reaction rate ω_{g} in Eq. (20) becomes zero, suggesting that fuel and oxygen do not coexist throughout the boundary layer and that the diffusion flame becomes a flame sheet.
2. In the limit of an infinitesimally thin reaction zone, by conducting an integration of the coupling function for CO and O_2 across the zone, bounded between $\eta_{f-} < \eta < \eta_{f+}$, where η_f is the location of flame sheet, we have

$$-\left(\frac{d\widetilde{Y}_{\mathrm{F}}}{d\eta}\right)_{f-} = \left(\frac{d\widetilde{Y}_{\mathrm{O}}}{d\eta}\right)_{f+} \quad \text{or} \quad -\left(\frac{dY_{\mathrm{F}}}{d\eta}\right)_{f-} = \frac{\nu_{\mathrm{F}}W_{\mathrm{F}}}{\nu_{\mathrm{O}}W_{\mathrm{O}}}\left(\frac{dY_{\mathrm{O}}}{d\eta}\right)_{f+}, \tag{51}$$

   suggesting that fuel and oxidizer must flow into the flame surface in stoichiometric proportions. Here the subscript $f+$ and $f-$, respectively, designate the oxygen and fuel sides of the flame. Note that in deriving Eq. (51), use has been made of an assumption that values of the individual quantities, such as the streamfunction f and species mass-fraction Y_i, can be continuous across the flame.
3. Similarly, by evaluating the coupling function for CO and enthalpy, we have

$$\left(\frac{d\widetilde{T}}{d\eta}\right)_{f-} - \left(\frac{d\widetilde{T}}{d\eta}\right)_{f+} = -\left(\frac{d\widetilde{Y}_{\mathrm{F}}}{d\eta}\right)_{f-} \quad \text{or} \quad \lambda\left(\frac{dT}{d\eta}\right)_{f-} - \lambda\left(\frac{dT}{d\eta}\right)_{f+} = -q\rho D\left(\frac{dY_{\mathrm{F}}}{d\eta}\right)_{f-}, \tag{52}$$

   suggesting that the amount of heat generated is equal to the heat, conducted away to the both sides of the reaction zone.

3.3 Flame-attached mode

When the surface reactivity is decreased by decreasing the surface temperature, then the detached flame sheet moves towards the surface until it is contiguous to it ($\xi_f = 0$). This critical state is given by the condition

$$\beta_a = \frac{\widetilde{Y}_{O,\infty}}{2\delta}, \tag{53}$$

obtained from Eq. (48), and defines the transition from the detached to the attached mode of the flame. Subsequent combustion with the Flame-attached mode is characterized by $Y_{F,s} = 0$ and $Y_{O,s} \geq 0$ (Libby & Blake, 1979; Makino & Law, 1986; Henriksen, et al., 1988), with the gas-phase temperature profile

$$\widetilde{T} = \widetilde{T}_s + \left(\widetilde{T}_\infty - \widetilde{T}_s\right)\xi, \tag{54}$$

given by the same relation as that for the frozen case, because all gas-phase reaction is now confined at the surface. By using the coupling functions in Eqs. (33) to (36) with $Y_{F,s} = 0$, it can be shown that

$$\delta\left(-f_s\right) = A_{s,O}\frac{\widetilde{Y}_{O,\infty} - 2\delta\beta}{1+\beta} + A_{s,P}\frac{\widetilde{Y}_{P,\infty} + \delta\beta}{1+\beta}. \tag{55}$$

which is also to be solved numerically from Eq. (15). The maximum combustion rate of this mode occurs at the transition state in Eq. (53), which also corresponds to the minimum combustion rate of the Flame-detached mode.

3.4 Diffusion-limited combustion rate

The maximum, diffusion-limited transfer number of the system can be achieved through one of the two limiting situations. The first appears when both of the surface reactions occur infinitely fast such that $Y_{O,s}$ and $Y_{P,s}$ both vanish, yielding Eq. (45). The second appears when the surface C-CO_2 reaction occurs infinitely fast in the limit of the Flame-detached mode, which again yields Eq. (45). It is of interest to note that in the first situation the reactivity of the gas-phase CO-O_2 reaction is irrelevant, whereas in the second the reactivity of the surface C-O_2 reaction is irrelevant. While the transfer numbers β are the same in both cases, the combustion rates, thereby the oxygen supply rates, are slightly different each other, as shown in Fig, 1(b), because of the different density coupling, related to the flame structures. Note that the limiting solutions identified herein provide the counterparts of those previously derived (Libby & Blake, 1979; Makino & Law, 1986) for the carbon particle, and generalize the solution of Matsui & Tsuji (1987) with including the surface C-CO_2 reaction.

4. Combustion rate and flame structure

A momentary reduction in the combustion rate, reported in theoretical works (Adomeit, et al., 1985; Makino & Law, 1986; Matsui & Tsuji, 1987; Henriksen, 1989; Makino, 1990; Makino & Law, 1990), can actually be exaggerated by the appearance of CO-flame in the gas phase, bringing about a change of the dominant surface reactions from the faster C-O_2 reaction to the slower C-CO_2 reaction, due to an intimate coupling between the surface and gas-phase

reactions. In spite of this theoretical accomplishment, there are very few experimental data that can support it.

In the literature, in general, emphasis has been put on examination of the surface reactivities with gaseous oxidizers, such as O_2, CO_2, and H_2O (*cf.* Essenhigh, 1981) although surface reactivities on the same solid carbon are limited (Khitrin & Golovina, 1964; Visser & Adomeit, 1984; Harris & Smith, 1990). As for the gas-phase CO-O_2 reactivity, which is sensitive to the H_2O concentration, main concern has been put on that of the CO-flame (Howard, et al., 1973), called the "strong" CO-oxidation, which is, however, far from the situation over the burning carbon, especially for that prior to the appearance of CO-flame, because some of the elementary reactions are too slow to sustain the "strong" CO-oxidation. Furthermore, it has been quite rare to conduct experimental studies from the viewpoint that there exist interactions between chemical reactions and flow, so that studies have mainly been confined to obtaining combustion rate (Khitrin & Golovina, 1964; Visser & Adomeit, 1984; Matsui, et al., 1975; Matsui, et al., 1983, 1986).

In order to examine such interactions, an attempt has been made to measure temperature profiles over the burning graphite rod in the forward stagnation flowfield (Makino, et al., 1996). In this measurement, N_2-CARS[2] thermometry (Eckbreth, 1988) is used in order to avoid undesired appearance and/or disappearance of the CO-flame. Not only the influence due to the appearance of CO-flame on the temperature profile, but also that on the combustion rate is investigated. Measured results are further compared with predicted results (Makino, 1990; Makino & Law, 1990; Makino, et al., 1994).

4.1 Combustion rate and ignition surface-temperature

Here, experimental results for the combustion rate and the temperature profiles in the gas phase are first presented, which are closely related to the coupled nature of the surface and gas-phase reactions. The experimental setup is schematically shown in Fig. 2. Air used as an oxidizer is supplied by a compressor and passes through a refrigerator-type dryer and a surge tank. The dew point from which the H_2O concentration is determined is measured by a hygrometer. The airflow at room temperature, after passing through a settling chamber (52.8 mm in diameter and 790 mm in length), issues into the atmosphere with a uniform velocity (up to 3 m/s), and impinges on a graphite rod to establish a two-dimensional stagnation flow. This flowfield is well-established and is specified uniquely by the velocity gradient a (=$4V_\infty/d$), where V_∞ is the freestream velocity and d the diameter of the graphite rod. The rod is Joule-heated by an alternating current (12 V; up to 1625 A). The surface temperature is measured by a two-color pyrometer. The temperature in the central part (about 10 mm in length) of the test specimen is nearly uniform. In experiment, the test specimen is set to burn in airflow at constant surface temperature during each experimental run. Since the surface temperature is kept constant with external heating, quasi-steady combustion can be accomplished. The experiment involves recording image of test specimen in the forward stagnation region by a video camera and analyzing the signal displayed on a TV monitor to obtain surface regression rate, which is used to determine the combustion rate, after having examined its linearity on the combustion time.

Figure 2(a) shows the combustion rate in airflow of 110 s^{-1} (Makino, et al., 1996), as a function of the surface temperature, when the H_2O mass-fraction is 0.003. The combustion rate, obtained from the regression rate and density change of the test specimen, increases

[2] CARS: Coherent Anti-Stokes Raman Spectroscopy

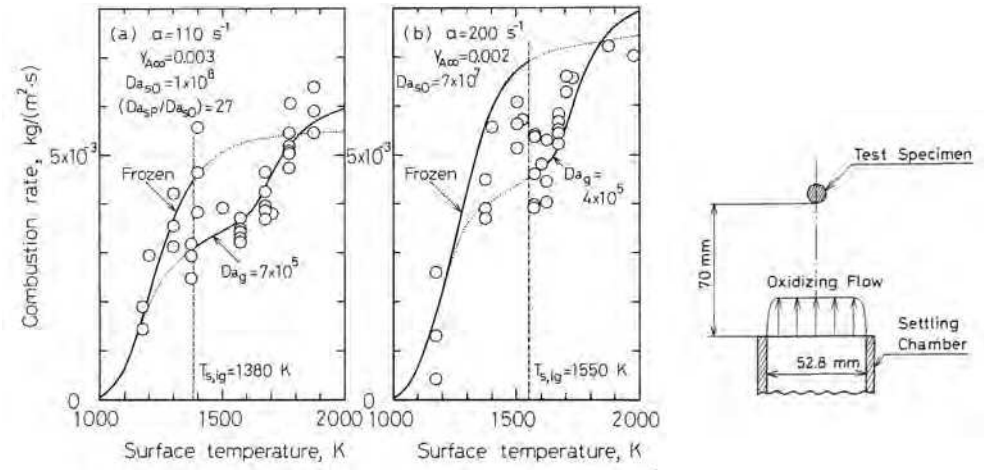

Fig. 2. Combustion rate of graphite rod (ρ_C=1.25×10³ kg/m³) as a function of the surface temperature; (a) for the velocity gradient of 110 s^{-1} in airflow with the H_2O mass-fraction of 0.003; (b) for the velocity gradient of 200 s^{-1} in airflow with the H_2O mass-fraction of 0.002. Data points are experimental (Makino, et al., 1996) and curves are calculated for the theory (Makino, 1990). The gas-phase Damköhler number corresponds to that for the "strong" CO-oxidation. The ignition surface-temperature $T_{s,ig}$ is calculated, based on the ignition analysis (Makino & Law, 1990). Schematical drawing of the experimental setup is also shown.

with increasing surface temperature, up to a certain surface temperature. The combustion in this temperature range is that with negligible CO-oxidation, and hence the combustion rate in Frozen mode can fairly predict the experimental results. A further increase in the surface temperature causes the momentary reduction in the combustion rate, because appearance of the CO-flame alters the dominant surface reaction from the C-O_2 reaction to the C-CO_2 reaction. The surface temperature when the CO-flame first appears is called the ignition surface-temperature (Makino & Law, 1990), above which the combustion proceeds with the "strong" CO-oxidation. The solid curve is the predicted combustion rate with the surface kinetic parameters (Makino, et al., 1994) to be explained in the next Section, and the global gas-phase kinetic parameters (Howard, et al., 1973). In numerical calculations, use has been made of the formulation, presented in Section 2.

The same trend is also observed in airflow of 200 s^{-1}, as shown in Fig. 2(b). Because of the reduced thickness of the boundary layer with respect to the oxidizer concentration, the combustion rate at a given surface temperature is enhanced. The ignition surface-temperature is raised because establishment of the CO-flame is suppressed, due to an increase in the velocity gradient.

4.2 Temperature profile in the gas phase

Temperature profiles in the forward stagnation region are shown in Fig. 3(a) when the velocity gradient of airflow is 110 s^{-1} and the H_2O mass-fraction is 0.002. The surface temperature is taken as a parameter, being controlled not to exceed ±20 K from a given value. We see that the temperature profile below the ignition surface-temperature (*ca.* 1450 K) is completely different from that above the ignition surface-temperature. When the

surface temperature is 1400 K, the gas-phase temperature monotonically decreases, suggesting negligible gas-phase reaction. When the surface temperature is 1500 K, at which CO-flame can be observed visually, there exists a reaction zone in the gas phase whose temperature is nearly equal to the surface temperature. Outside the reaction zone, the temperature gradually decreases to the freestream temperature. When the surface temperature is 1700 K, the gas-phase temperature first increases from the surface temperature to the maximum, and then decreases to the freestream temperature. The existence of the maximum temperature suggests that a reaction zone locates away from the surface. That is, a change of the flame structures has certainly occurred upon the establishment of CO-flame.

It may be informative to note the advantage of the CARS thermometry over the conventional, physical probing method with thermocouple. When the thermocouple is used for the measurement of temperature profile corresponding to the surface temperature of 1400 K (or 1500 K), it distorts the combustion field, and hence makes the CO-flame appear (or disappear). In this context, the present result suggests the importance of using thermometry without disturbing the combustion fields, especially for the measurement at the ignition/extinction of CO-flame. In addition, the present results demonstrate the high spatial resolution of the CARS thermometry, so that the temperature profile within a thin boundary layer of a few mm can be measured.

Predicted results are also shown in Fig. 3(a). In numerical calculations, use has been made of the formulation mentioned in Section 2 and kinetic parameters (Makino, et al., 1994) to be explained in the next Section. When there exists CO-flame, the gas-phase kinetic parameters used are those for the "strong" CO-oxidation; when the CO-oxidation is too weak to establish the CO-flame, those for the "weak" CO-oxidation are used. Fair agreement between experimental and predicted results is shown, if we take account of measurement errors (±50 K) in the present CARS thermometry.

Our choice of the global gas-phase chemistry requires a further comment, because nowadays it is common to use detailed chemistry in the gas phase. Nonetheless, because of its simplicity, it is decided to use the global gas-phase chemistry, after having examined the fact that the formulation with detailed chemistry (Chelliah, et al., 1996) offers nearly the same results as those with global gas-phase chemistry.

Figure 3(b) shows the temperature profiles for the airflow of 200 s^{-1}. Because of the increased velocity gradient, the ignition surface-temperature is raised to be *ca.* 1550 K, and the boundary-layer thickness is contracted, compared to Fig. 3(a), while the general trend is the same.

Figure 3(c) shows the temperature profiles at the surface temperature 1700 K, with the velocity gradient of airflow taken as a parameter (Makino, et al., 1997). It is seen that the flame structure shifts from that with high temperature flame zone in the gas phase to that with gradual decrease in the temperature, suggesting that the establishment of CO-flame can be suppressed with increasing velocity gradient.

Note here that in obtaining data in Figs. 3(a) to 3(c), attention has been paid to controlling the surface temperature not to exceed ±20 K from a given value. In addition, the surface temperature is intentionally set to be lower (or higher) than the ignition surface-temperature by 20 K or more. If we remove these restrictions, results are somewhat confusing and gas-phase temperature scatters in relatively wide range, because of the appearance of unsteady combustion (Kurylko & Essenhigh, 1973) that proceeds without CO-flame at one time, while with CO-flame at the other time.

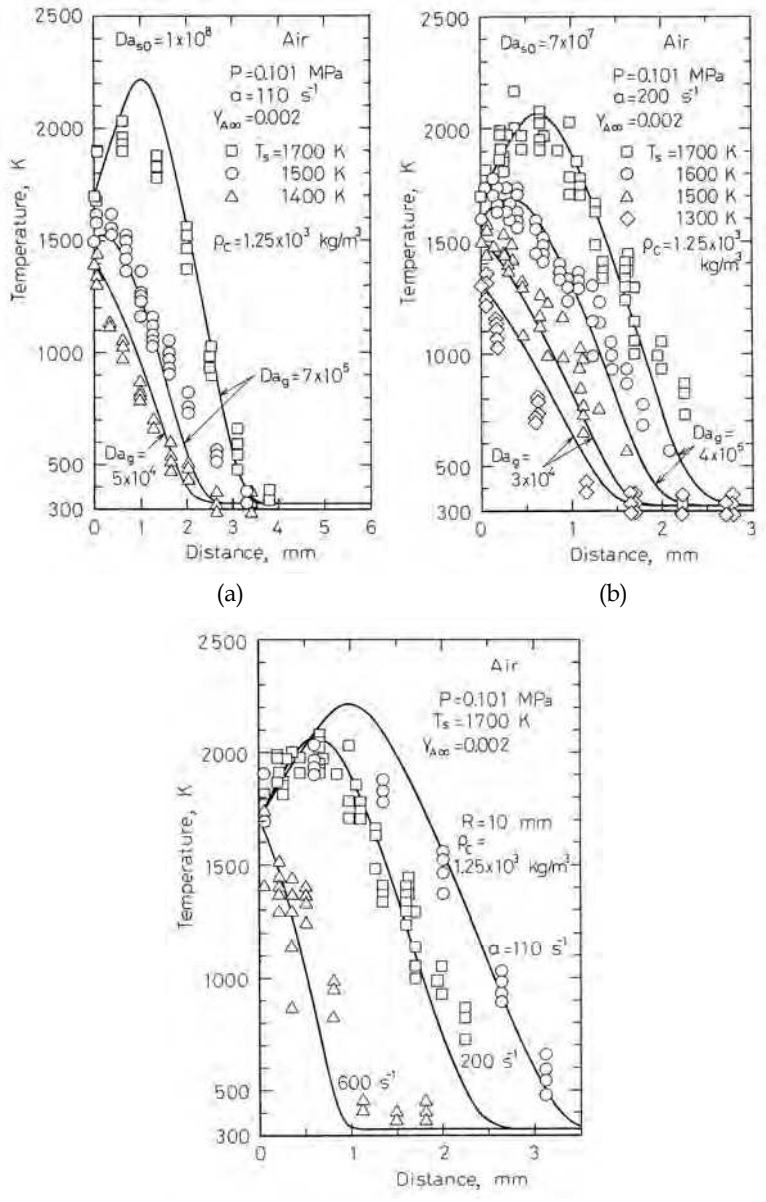

Fig. 3. Temperature profiles over the burning graphite rod in airflow at an atmospheric pressure. The H_2O mass-fraction is 0.002. Data points are experimental (Makino, et al., 1996; Makino, et al., 1997) and solid curves are theoretical (Makino, 1990); (a) for the velocity gradient 110 s^{-1}, with the surface temperature taken as a parameter; (b) for 200 s^{-1}; (c) for the surface temperature 1700 K, with the velocity gradient taken as a parameter.

4.3 Ignition criterion

While studies relevant to the ignition/extinction of CO-flame over the burning carbon are of obvious practical utility in evaluating protection properties from oxidation in re-entry vehicles, as well as the combustion of coal/char, they also command fundamental interests because of the simultaneous existence of the surface and gas-phase reactions with intimate coupling (Visser & Adomeit, 1984; Makino & Law, 1986; Matsui & Tsuji, 1987). As mentioned in the previous Section, at the same surface temperature, the combustion rate is expected to be momentarily reduced upon ignition because establishment of the CO-flame in the gas phase can change the dominant surface reactions from the faster C-O_2 reaction to the slower C-CO_2 reaction. By the same token the combustion rate is expected to momentarily increase upon extinction. These concepts are not intuitively obvious without considering the coupled nature of the gas-phase and surface reactions.

Fundamentally, the ignition/extinction of CO-flame in carbon combustion must necessarily be described by the seminal analysis (Liñán, 1974) of the ignition, extinction, and structure of diffusion flames, as indicated by Matalon (1980, 1981, 1982). Specifically, as the flame temperature increases from the surface temperature to the adiabatic flame temperature, there appear a nearly-frozen regime, a partial-burning regime, a premixed-flame regime, and finally a near-equilibrium regime. Ignition can be described in the nearly-frozen regime, while extinction in the other three regimes.

For carbon combustion, Matalon (1981) analytically obtained an explicit ignition criterion when the O_2 mass-fraction at the surface is O(l). When this concentration is O(ε), the appropriate reduced governing equation and the boundary conditions were also identified (Matalon, 1982). Here, putting emphasis on the ignition of CO-flame over the burning carbon, an attempt has first been made to extend the previous theoretical studies, so as to include analytical derivations of various criteria governing the ignition, with arbitrary O_2 concentration at the surface. Note that these derivations are successfully conducted, by virtue of the generalized species-enthalpy coupling functions (Makino & Law, 1986; Makino, 1990), identified in the previous Section. Furthermore, it may be noted that the ignition analysis is especially relevant for situations where the surface O_2 concentration is O(ε) because in order for gas-phase reaction to be initiated, sufficient amount of carbon monoxide should be generated. This requires a reasonably fast surface reaction and thereby low O_2 concentration. The second objective is to conduct experimental comparisons relevant to the ignition of CO-flame over a carbon rod in an oxidizing stagnation flow, with variations in the surface temperature of the rod, as well as the freestream velocity gradient and O_2 concentration.

4.3.1 Ignition analysis

Here we intend to obtain an explicit ignition criterion without restricting the order of $Y_{O,s}$. First we note that in the limit of $Ta_g \to \infty$, the completely frozen solutions for Eqs. (16) and (17) are

$$\left(\tilde{T}\right)_0 = \tilde{T}_s + \left(\tilde{T}_\infty - \tilde{T}_s\right)\xi \tag{56}$$

$$\left(\tilde{Y}_i\right)_0 = \tilde{Y}_{i,s} + \left(\tilde{Y}_{i,\infty} - \tilde{Y}_{i,s}\right)\xi \qquad (i = \mathrm{F, O, P}) \tag{57}$$

For finite but large values of Ta_g, weak chemical reaction occurs in a thin region next to the carbon surface when the surface temperature is moderately high and exceeds the ambient

temperature. Since the usual carbon combustion proceeds under this situation, corresponding to the condition (Liñán, 1974) of

$$\tilde{T}_s + \tilde{Y}_{F,s} > \tilde{T}_\infty , \tag{58}$$

we define the inner temperature distribution as

$$\left(\tilde{T}\right)_{in} = \left(\tilde{T}\right)_0 + \varepsilon\, \tilde{T}_s \lambda\theta(\xi) + O\left(\varepsilon^2\right) = \tilde{T}_s\left[1 - \varepsilon(\chi - \lambda\theta)\right] + O\left(\varepsilon^2\right) \tag{59}$$

where

$$\varepsilon = \frac{\tilde{T}_s}{\tilde{T}a_g}, \quad \lambda = \frac{\tilde{Y}_{O,\infty}}{\tilde{T}_s - \tilde{T}_\infty}, \quad \xi = \varepsilon\left(\frac{\tilde{T}_s}{\tilde{T}_s - \tilde{T}_\infty}\right)\chi . \tag{60}$$

In the above, ε is the appropriate small parameter for expansion, and χ and θ are the inner variables.

With Eq. (59) and the coupling functions of Eqs. (33) to (36), the inner species distributions are given by:

$$\left(\tilde{Y}_O\right)_{in} = \tilde{Y}_{O,s} + \varepsilon\, \tilde{T}_s \lambda(\chi - \theta) \tag{61}$$

$$\left(\tilde{Y}_F\right)_{in} = \left(\frac{2\delta\beta - \tilde{Y}_{O,\infty}}{1+\beta}\right) + \tilde{Y}_{O,s} + \varepsilon\left(\frac{\tilde{T}_s}{\tilde{T}_s - \tilde{T}_\infty}\right)\left(\frac{\tilde{Y}_{O,\infty} - 2\delta\beta}{1+\beta}\chi - \tilde{Y}_{O,\infty}\theta\right). \tag{62}$$

Thus, through evaluation of the parameter γ, expressed as

$$\gamma \equiv \left(\frac{d\tilde{T}}{d\xi}\right)_s = \left[\frac{d\chi}{d\xi}\frac{d\left(\tilde{T}\right)_{in}}{d\chi}\right]_s = -\left(\tilde{T}_s - \tilde{T}_\infty\right) + \tilde{Y}_{O,\infty}\left(\frac{d\theta}{d\chi}\right)_s + O(\varepsilon), \tag{63}$$

the O_2 mass-fraction at the surface is obtained as

$$\tilde{Y}_{O,s} = \frac{\tilde{Y}_{O,\infty}}{1 + \beta + A_{s,O}\left[\beta/\left(-f_s\right)\right]}\left\{1 - \left(\frac{d\theta}{d\chi}\right)_s\right\}. \tag{64}$$

Substituting χ, Eqs. (59), (61), and (62) into the governing Eq. (17), expanding, and neglecting the higher-order convection terms, we obtain

$$\frac{d^2\theta}{d\chi^2} = -\Delta(\chi - \theta + \eta_O)^{1/2}\exp(\lambda\theta - \chi), \tag{65}$$

where

$$\Delta = Da_g \exp\left(-\frac{\tilde{T}a_g}{\tilde{T}_s}\right)\left\{\left(\frac{\beta}{\left(-f_s\right)}\right)\left(\frac{\tilde{T}_s}{\tilde{T}_s - \tilde{T}_\infty}\right)\right\}^2\left(\frac{\tilde{T}_s}{\tilde{T}a_g}\right)^{3/2}\left(\frac{\tilde{T}_\infty}{\tilde{T}_s}\right)^{1/2}\frac{\tilde{Y}_{F,s}}{\left(\lambda\tilde{T}_s\right)^{1/2}}, \tag{66}$$

$$\eta_O = \frac{\tilde{Y}_{O,s}}{\varepsilon \tilde{T}_s \lambda}. \tag{67}$$

Note that the situation of $Y_{F,s}$ = O(ε) is not considered here because it corresponds to very weak carbon combustion, such as in low O_2 concentration or at low surface temperature.
Evaluating the inner temperature at the surface of constant T_s, one boundary condition for Eq. (65) is

$$\theta(0)=0 \tag{68}$$

This boundary condition is a reasonable one from the viewpoint of gas-phase quasi-steadiness in that its surface temperature changes at rates much slower than that of the gas phase, since solid phase has great thermal inertia.
For the outer, non-reactive region, if we write

$$\left(\tilde{T}\right)_{\text{out}} = \tilde{T}_s + \left(\tilde{T}_\infty - \tilde{T}_s\right)\xi + \varepsilon\, \tilde{T}_s \Theta(\xi) + O\left(\varepsilon^2\right), \tag{69}$$

we see from Eq. (17) that Θ is governed by $\mathcal{L}(\Theta)=0$ with the boundary condition that Θ (∞) = 0. Then, the solution is $\Theta(\xi) = - C_I (1 - \xi)$, where C_I is a constant to be determined through matching.
By matching the inner and outer temperatures presented in Eqs. (59) and (69), respectively, we have

$$\lambda\theta(\infty) = -C_I, \qquad \left(\frac{d\theta}{d\chi}\right)_\infty = 0. \tag{70}$$

the latter of which provides the additional boundary condition to solve Eq. (65), while the former allows the determination of C_I.
Thus the problem is reduced to solving the single governing Eq. (65), subject to the boundary conditions Eqs. (68) and (70). The key parameters are Δ, λ, and η_O. Before solving Eq. (65) numerically, it should be noted that there exists a general expression for the ignition criterion as

$$2\Delta_I\lambda = \frac{1}{\sqrt{\eta_O} + \frac{\sqrt{\pi/\lambda}}{2} e^{\lambda\eta_O}\left\{erfc(\lambda\eta_O) + (\lambda-1)\int_{\chi_1}^{\infty} e^{(\lambda-1)\chi} erfc(z)d\chi\right\}}; \quad erfc(z) = \frac{2}{\sqrt{\pi}}\int_z^\infty \exp\left(-t^2\right)dt, \tag{71}$$

corresponding to the critical condition for the vanishment of solutions at

$$\left(\frac{d\theta}{d\chi}\right)_s = \frac{1}{\lambda} \quad \text{or} \quad \left(\frac{d\left(\tilde{T}\right)_{in}}{d\xi}\right)_s = 0, \tag{72}$$

which implies that the heat transferred from the surface to the gas phase ceases at the ignition point. Note also that Eq. (71) further yields analytical solutions for some special cases, such as

$$\text{at } \lambda = 1: \quad 2\Delta_I = \frac{1}{\sqrt{\eta_O} + \frac{\sqrt{\pi}}{2} e^{\eta_O} erfc(\lambda\eta_O)}, \tag{73}$$

$$\text{as } \eta_O \to \infty: \quad 2\Delta_I \lambda = \frac{1}{\sqrt{\eta_O}}, \tag{74}$$

the latter of which agrees with the result of Matalon (1981).
In numerically solving Eq. (65), by plotting $\theta(\infty)$ vs. Δ for a given set of λ and η_O, the lower ignition branch of the S-curve can first be obtained. The values of Δ, corresponding to the vertical tangents to these curves, are then obtained as the reduced ignition Damköhler number Δ_I. After that, a universal curve of $(2\Delta_I\lambda)$ vs. $(1/\lambda)$ is obtained with η_O taken as a parameter. Recognizing that $(1/\lambda)$ is usually less than about 0.5 for practical systems and using Eqs. (71), (73), and (74), we can fairly represent $(2\Delta_I\lambda)$ as (Makino & Law, 1990)

$$2\Delta_I \lambda = \frac{1}{\sqrt{\eta_O} + \frac{\sqrt{\pi}}{2}\left[e^{\eta_O}\, erfc\left(\sqrt{\eta_O}\right) + \left\{ \frac{1}{F(\lambda)} - 1 \right\} \exp\left(-\frac{\sqrt{\eta_O}}{2} \right) \right]}, \tag{75}$$

where

$$F(\lambda) = 0.56 + \frac{0.21}{\lambda} - \frac{0.12}{\lambda^2} + \frac{0.35}{\lambda^3} \tag{76}$$

Note that for large values of $(1/\lambda)$, Eq. (75) is still moderately accurate. Thus, for a given set of λ and η_O, an ignition Damköhler number can be determined by substituting the values of Δ_I, obtained from Eq. (75), into Eq. (66).
It may be informative to note that for some weakly-burning situations, in which O_2 concentrations in the reaction zone and at the carbon surface are O(1), a monotonic transition from the nearly-frozen to the partial-burning behaviors is reported (Henriksen, 1989), instead of an abrupt, turning-point behavior, with increasing gas-phase Damköhler number. However, this could be a highly-limiting behavior. That is, in order for the gas-phase reaction to be sufficiently efficient, and the ignition to be a reasonably plausible event, enough CO would have to be generated at the surface, which further requires a sufficiently fast surface C-O_2 reaction and hence the diminishment of the surface O_2 concentration from O(l). For these situations, the turning-point behavior can be a more appropriate indication for the ignition.

4.3.2 Experimental comparisons for the ignition of CO flame

Figure 4 shows the ignition surface-temperature (Makino, et al., 1996), as a function of the velocity gradient, with O_2 mass-fraction taken as a parameter. The velocity gradient has been chosen for the abscissa, as originally proposed by Tsuji & Yamaoka (1967) for the present flow configuration, after confirming its appropriateness, being examined by varying both the freestream velocity and graphite rod diameter that can exert influences in determining velocity gradient. It is seen that the ignition surface-temperature increases with increasing velocity gradient and thereby decreasing residence time. The high surface temperature, as well as the high temperature in the reaction zone, causes the high ejection rate of CO through the surface C-O_2 reaction. These enhancements facilitate the CO-flame, by reducing the characteristic chemical reaction time, and hence compensating a decrease in the characteristic residence time. It is also seen that the ignition surface-temperature

decreases with increasing $Y_{O,\infty}$. In this case the CO-O_2 reaction is facilitated with increasing concentrations of O_2, as well as CO, because more CO is now produced through the surface C-O_2 reaction.

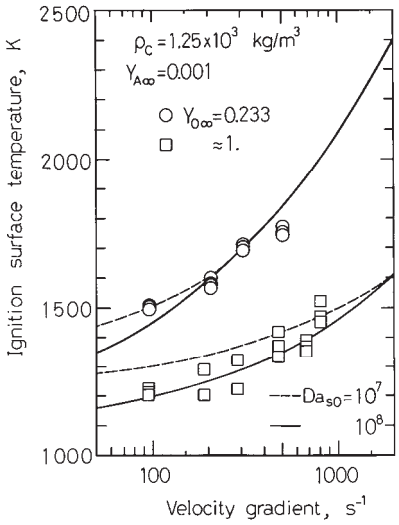

Fig. 4. Surface temperature at the establishment of CO-flame, as a function of the stagnation velocity gradient, with the O_2 mass-fraction in the freestream and the surface Damköhler number for the C-O_2 reaction taken as parameters. Data points are experimental (Makino, et al., 1996) with the test specimen of 10 mm in diameter and 1.25×10^3 kg/m^3 in graphite density; curves are calculated from theory (Makino & Law, 1990).

Solid and dashed curves in Fig. 4 are predicted ignition surface-temperature for $Da_{s,O}=10^7$ and 10^8, obtained by the ignition criterion described here and the kinetic parameters (Makino, et al., 1994) to be explained, with keeping as many parameters fixed as possible. The density ρ_∞ of the oxidizing gas in the freestream is estimated at T_∞= 323 K. The surface Damköhler numbers in the experimental conditions are from 2×10^7 to 2×10^8, which are obtained with $B_{s,O}$ = 4.1×10^6 m/s. It is seen that fair agreement is demonstrated, suggesting that the present ignition criterion has captured the essential feature of the ignition of CO-flame over the burning carbon.

5. Kinetic parameters for the surface and gas-phase reactions

In this Section, an attempt is made to extend and integrate previous theoretical studies (Makino, 1990; Makino and Law, 1990), in order to further investigate the coupled nature of the surface and gas-phase reactions. First, by use of the combustion rate of the graphite rod in the forward stagnation region of various oxidizer-flows, it is intended to obtain kinetic parameters for the surface C-O_2 and C-CO_2 reactions, based on the theoretical work (Makino, 1990), presented in Section 2. Second, based on experimental facts that the ignition of CO-flame over the burning graphite is closely related to the surface temperature and the

stagnation velocity gradient, it is intended to obtain kinetic parameters for the global gas-phase CO-O_2 reaction prior to the ignition of CO-flame, by use of the ignition criterion (Makino and Law, 1990), presented in Section 4. Finally, experimental comparisons are further to be conducted.

5.1 Surface kinetic parameters

In estimating kinetic parameters for the surface reactions, their contributions to the combustion rate are to be identified, taking account of the combustion situation in the limiting cases, as well as relative reactivities of the C-O_2 and C-CO_2 reactions. In the kinetically controlled regime, the combustion rate reflects the surface reactivity of the ambient oxidizer. Thus, by use of Eqs. (31) and (34), the reduced surface Damköhler number is expressed as

$$A_i = \frac{\delta(-f_s)(1+\beta)}{\tilde{Y}_{i,\infty} - \delta\beta} \qquad (i = \mathrm{O}, \mathrm{P}) \tag{77}$$

when only one kind of oxidizer participates in the surface reaction.
In the diffusionally controlled regime, combustion situation is that of the Flame-detached mode, thereby following expression is obtained:

$$A_\mathrm{P} = \frac{\delta(-f_s)(1+\beta)}{\tilde{Y}_{\mathrm{O},\infty} - \delta\beta} \tag{78}$$

Note that the combustion rate here reflects the C-CO_2 reaction even though there only exists oxygen in the freestream.

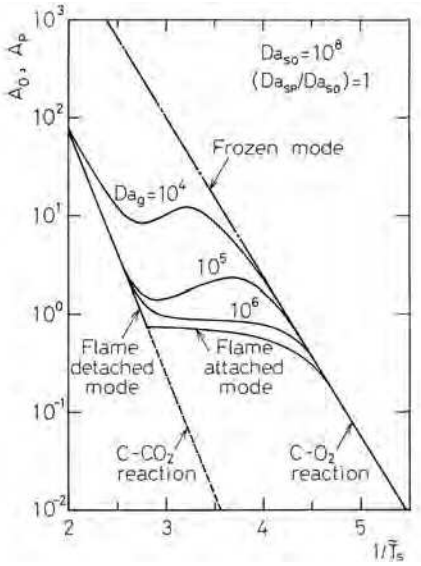

Fig. 5. Arrhenius plot of the reduced surface Damköhler number with the gas-phase Damköhler number taken as a parameter; $Da_{s,O}$= $Da_{s,P}$=10^8; $Da_{s,P}/Da_{s,O}$=1; $Y_{O,\infty}$=0.233; $Y_{P,\infty}$=0 (Makino, et al., 1994).

In order to verify this method, the reduced surface Damköhler number A_i is obtained numerically by use of Eq. (77) and/or Eq. (78). Figure 5 shows the Arrhenius plot of A_i with the gas-phase Damköhler number taken as a parameter. We see that with increasing surface temperature the combustion behavior shifts from the Frozen mode to the Flame-detached mode, depending on the gas-phase Damköhler number. Furthermore, in the present plot, the combustion behavior in the Frozen mode purely depends on the surface C-O_2 reaction rate; that in the Flame-detached mode depends on the surface C-CO_2 reaction rate. Since the appropriateness of the present method has been demonstrated, estimation of the surface kinetic parameters is conducted with experimental results (Makino, et al., 1994), by use of an approximate relation (Makino, 1990)

$$\left(\xi_s'\right) = 0.4\tilde{T}_s + 0.56 \tag{79}$$

for evaluating the transfer number β from the combustion rate through the relation $\beta=(-f_s)/(\xi'_s)$ in Eq. (39). Values of parameters used are q = 10.11 MJ/kg, c_p = 1.194 kJ/(kg·K), $q/(c_p\alpha_F)$ = 5387 K, and T_∞ = 323 K. Thermophysical properties of oxidizer are also conventional ones (Makino, et al., 1994).

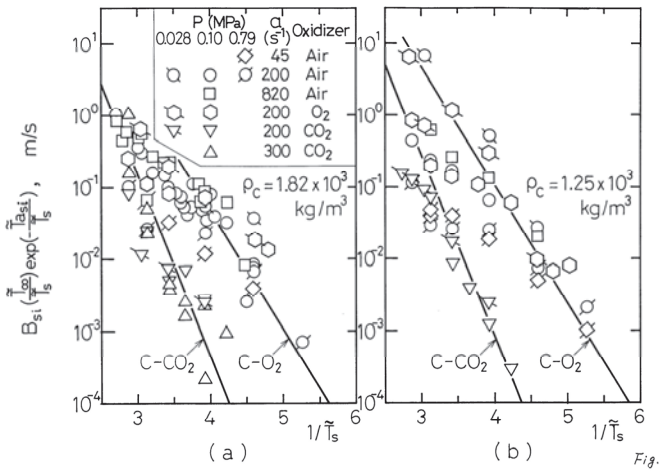

Fig. 6. Arrhenius plot of the surface C-O_2 and C-CO_2 reactions (Makino, et al., 1994), obtained from the experimental results of the combustion rate in oxidizer-flow of various velocity gradients; (a) for the test specimen of 1.82×10^3 kg/m^3 in graphite density; (b) for the test specimen of 1.25×10^3 kg/m^3 in graphite density.

Figure 6(a) shows the Arrhenius plot of surface reactivities, being obtained by multiplying A_i by $[a(\mu_\infty/\rho_\infty)]^{1/2}$, for the results of the test specimen with 1.82×10^3 kg/m^3 in density. For the C-O_2 reaction $B_{s,O}$ =2.2×10^6 m/s and $E_{s,O}$ = 180 kJ/mol are obtained, while for the C-CO_2 reaction $B_{s,P}$ = 6.0×10^7 m/s and $E_{s,P}$ = 269 kJ/mol. Figure 6(b) shows the results of the test specimen with 1.25×10^3 kg/m^3. It is obtained that $B_{s,O}$ = 4.1×10^6 m/s and $E_{s,O}$= 179 kJ/mol for the C-O_2 reaction, and that $B_{s,P}$ = 1.1×10^8 m/s and $E_{s,P}$ = 270 kJ/mol for the C-CO_2 reaction. Activation energies are respectively within the ranges of the surface C-O_2 and C-

CO_2 reactions; *cf.* Table 19.6 in Essenhigh (1981). It is also seen in Figs. 6(a) and 6(b) that the first-order Arrhenius kinetics, assumed in the theoretical model, is appropriate for the surface C-O_2 and C-CO_2 reactions within the present experimental conditions.

5.2 Global gas-phase kinetic parameters

Estimation of gas-phase kinetic parameters has also been made with experimental data for the ignition surface-temperature and the ignition criterion (Makino & Law, 1990) for the CO-flame over the burning carbon. Here, reaction orders are *a priori* assumed to be $n_F = 1$ and $n_O = 0.5$, which are the same as those of the global rate expression by Howard et al. (1973). It is also assumed that the frequency factor B_g is proportional to the half order of H_2O concentration: that is, $B_g = B_g^*(\rho Y_A/W_A)^{1/2}$ $[(\mathrm{mol/m^3})^{1/2}\cdot\mathrm{s}]^{-1}$, where the subscript A designates water vapor. The H_2O mass-fraction at the surface is estimated with $Y_{A,s} = Y_{A,\infty}/(1+\beta)$, with water vapor taken as an inert because it acts as a kind of catalyst for the gas-phase CO-O_2 reaction, and hence its profile is not anticipated to be influenced. Thus, for a given set of λ and η_O, an ignition Damköhler number can be determined by substituting Δ_I in Eq. (75) into Eq. (66).

Figure 7 shows the Arrhenius plot of the global gas-phase reactivity, obtained as the results of the ignition surface-temperature. In data processing, data in a series of experiments (Makino & Law, 1990; Makino, et al., 1994) have been used, with using kinetic parameters for the surface C-O_2 reaction. With iteration in terms of the activation temperature, required for determining Δ_I with respect to η_O, E_g = 113 kJ/mol is obtained with $B_g^* = 9.1\times10^6$ $[(\mathrm{mol/m^3})^{1/2}\cdot\mathrm{s}]^{-1}$. This activation energy is also within the range of the global CO-O_2 reaction; *cf.* Table II in Howard, et al. (1973).

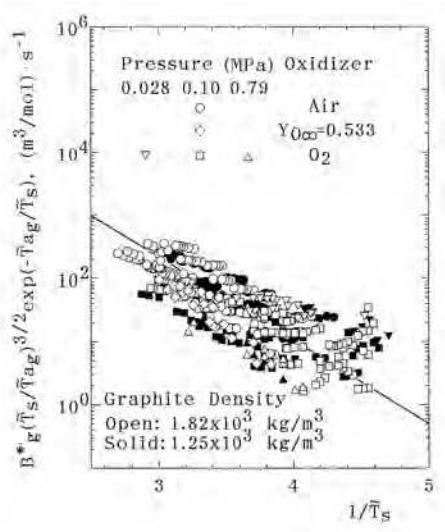

Fig. 7. Arrhenius plot of the global gas-phase reaction (Makino, et al., 1994), obtained from the experimental results of the ignition surface-temperature for the test specimens (1.82×10^3 kg/m^3 and 1.25×10^3 kg/m^3 in graphite density) in oxidizer-flow at various pressures, O_2, and H_2O concentrations .

It is noted that B_g* obtained here is one order of magnitude lower than that of Howard, et al. (1973), which is reported to be B_g* =1.3×10^8 [(mol/m^3)$^{1/2}$·s]$^{-1}$, because the present value is that prior to the appearance of CO-flame and is to be low, compared to that of the "strong" CO-oxidation in the literature. As for the "weak" CO-oxidation, Sobolev (1959) reports B_g* = 3.0×10^6 [(mol/m^3)$^{1/2}$·s]$^{-1}$, by examining data of Chukhanov (1938a, 1938b) who studied the initiation of CO-oxidation, accompanied by the carbon combustion. We see that the value reported by Sobolev (1959) exhibits a lower bound of the experimental results shown in Fig. 7. It is also confirmed in Fig. 7 that there exists no remarkable effects of O_2 and/or H_2O concentrations in the oxidizer, thereby the assumption for the reaction orders is shown to be appropriate within the present experimental conditions. The choice of reaction orders, however, requires a further comment because another reaction order for O_2 concentration, 0.25 in place of 0.5, is recommended in the literature. Relevant to this, an attempt (Makino, et al., 1994) has further been conducted to compare the experimental data with another ignition criterion, obtained through a similar ignition analysis with this reaction order. However, its result was unfavorable, presenting a much poorer correlation between them.

5.3 Experimental comparisons for the combustion rate

Experimental comparisons have already been conducted in Fig. 2, for test specimens with ρ_C=1.25×10^3 kg/m^3 in graphite density, and a fair degree of agreement has been demonstrated, as far as the trend and approximate magnitude are concerned. Further experimental comparisons are made for test specimens with ρ_C=1.82×10^3 kg/m^3 (Makino, et al., 1994), with kinetic parameters obtained herein. Figure 8(a) compares predicted results with experimental data in airflow of 200 s^{-1} at an atmospheric pressure. The gas-phase Damköhler number is evaluated to be Da_g= 3×10^4 from the present kinetic parameter, while Da_g = 4×10^5 from the value in the literature (Howard, et al., 1973). The ignition surface-temperature is estimated to be $T_{s,ig}$ ≈1476 K from the ignition analysis. We see from Fig. 8(a)

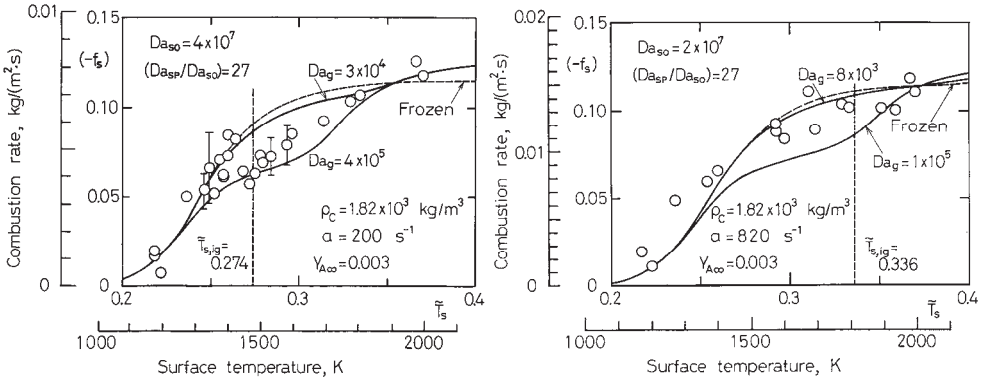

(a) (b)

Fig. 8. Experimental comparisons (Makino, et al., 1994) for the combustion rate of test specimen (ρ_C = 1.82×10^3 kg/m^3 in graphite density) in airflow under an atmospheric pressure with H_2O mass-fraction of 0.003; (a) for 200 s^{-1} in stagnation velocity gradient; (b) for 820 s^{-1}. Data points are experimental and solid curves are calculated from theory. The nondimensional temperature can be converted into conventional one by multiplying $q/(c_p\alpha_F)$ = 5387 K.

that up to the ignition surface-temperature the combustion proceeds under the "weak" CO-oxidation, that at the temperature the combustion rate abruptly changes, and that the "strong" CO-oxidation prevails above the temperature.
Figure 8(b) shows a similar plot in airflow of 820 s^{-1}. Because of the lack of the experimental data, as well as the enhanced ignition surface-temperature ($T_{s,ig} \approx 1810$ K), which inevitably leads to small difference between combustion rates before and after the ignition of CO-flame, the abrupt change in the combustion rate does not appear clearly. However, the general behavior is similar to that in Fig. 8(a).
It may informative to note that a decrease in the combustion rate, observed at temperatures between 1500 K and 2000 K, has been so-called the "negative temperature coefficient" of the combustion rate, which has also been a research subject in the field of carbon combustion. Nagel and Strickland-Constable (1962) used the "site" theory to explain the peak rate, while Yang and Steinberg (1977) attributed the peak rate to the change of reaction depth at constant activation energy. Other entries relevant to the "negative temperature coefficient" can be found in the survey paper (Essenhigh, 1981). However, another explanation can be made, as explained (Makino, et al., 1994; Makino, et al., 1996; Makino, et al., 1998) in the previous Sections, that this phenomenon can be induced by the appearance of CO-flame, established over the burning carbon, thereby the dominant surface reaction has been altered from the C-O_2 reaction to the C-CO_2 reaction.
Since the appearance of CO-flame is anticipated to be suppressed at high velocity gradients, it has strongly been required to raise the velocity gradient as high as possible, in order for firm understanding of the carbon combustion, while it has been usual to do experiments under the stagnation velocity gradient less than 1000 s^{-1} (Matsui, et al., 1975; Visser & Adomeit, 1984; Makino, et al., 1994; Makino, et al., 1996), because of difficulties in conducting experiments. In one of the Sections in Part 2, it is intended to study carbon combustion at high velocity gradients.

6. Concluding remarks of part 1

In this monograph, combustion of solid carbon has been overviewed not only experimentally but also theoretically. In order to have a clear understanding, only the carbon combustion in the forward stagnation flowfield has been considered here. In the formulation, an aerothermochemical analysis has been conducted, based on the chemically reacting boundary layer, with considering the surface C-O_2 and C-CO_2 reactions and the gas-phase CO-O_2 reaction. By virtue of the generalized species-enthalpy coupling functions, derived successfully, it has been demonstrated that there exists close coupling between the surface and gas-phase reactions that exerts influences on the combustion rate. Combustion response in the limiting situations has further been identified by using the generalized coupling functions.
After confirming the experimental fact that the combustion rate momentarily reduces upon ignition, because establishment of the CO-flame in the gas phase can change the dominant surface reaction from the faster C-O_2 reaction to the slower C-CO_2 reaction, focus has been put on the ignition of CO-flame over the burning carbon in the prescribed flowfield and theoretical studies have been conducted by using the generalized coupling functions. The asymptotic expansion method has been used to derive the explicit ignition criterion, from which in accordance with experimental results, it has been shown that ignition is facilitated with increasing surface temperature and oxidizer concentration, while suppressed with decreasing velocity gradient.

Then, attempts have been made to estimate kinetic parameters for the surface and gas-phase reactions, indispensable for predicting combustion behavior. In estimating the kinetic parameters for the surface reactions, use has been made of the reduced surface Damköhler number, evaluated by the combustion rate measured in experiments. In estimating the kinetic parameters for the global gas-phase reaction, prior to the appearance of the CO-flame, use has been made of the ignition criterion theoretically obtained, by evaluating it at the ignition surface-temperature experimentally determined. Experimental comparisons have also been conducted and a fair degree of agreement has been demonstrated between experimental and theoretical results.
Further studies are intended to be made in Part 2 for exploring carbon combustion at high velocity gradients and/or in the High-Temperature Air Combustion, in which effects of water-vapor in the oxidizing-gas are also to be taken into account.

7. Acknowledgment

In conducting a series of studies on the carbon combustion, I have been assisted by many of my former graduate and undergraduate students, as well as research staffs, in Shizuoka University, being engaged in researches in the field of mechanical engineering for twenty years as a staff, from a research associate to a full professor. Here, I want to express my sincere appreciation to all of them who have participated in researches for exploring combustion of solid carbon.

8. Nomenclature

General

A	reduced surface Damköhler number
a	velocity gradient in the stagnation flowfield
B	frequency factor
C	constant
c_p	specific heat capacity of gas
D	diffusion coefficient
Da	Damköhler number
d	diameter
E	activation energy
F	function defined in the ignition criterion
f	nondimensional streamfunction
j	j=0 and 1 designate two-dimensional and axisymmetric flows, respectively
k	surface reactivity
$\mathcal{L}$	convective-diffusive operator
$\dot{m}$	dimensional mass burning (or combustion) rate
q	heat of combustion per unit mass of CO
R^o	universal gas constant
R	curvature of surface or radius
s	boundary-layer variable along the surface
T	temperature
Ta	activation temperature
t	time

u velocity component along x
V freestream velocity
v velocity component along y
W molecular weight
w reaction rate
x tangential distance along the surface
Y mass fraction
y normal distance from the surface

Greek symbols

α stoichiometric CO_2-to-reactant mass ratio
β conventional transfer number
γ temperature gradient at the surface
Δ reduced gas-phase Damköhler number
δ product(CO_2)-to-carbon mass ratio
ε measure of the thermal energy in the reaction zone relative to the activation energy
η boundary-layer variable normal to the surface or perturbed concentration
Θ perturbed temperature in the outer region
θ perturbed temperature in the inner region
λ thermal conductivity or parameter defined in the ignition analysis
μ viscosity
ν stoichiometric coefficient
ξ profile function
ρ density
χ inner variable
ψ streamfunction
ω reaction rate

Subscripts

A water vapor or C-H_2O surface reaction
a critical value at flame attachment
C carbon
F carbon monoxide
f flame sheet
g gas phase
ig ignition
in inner region
max maximum value
N nitrogen
O oxygen or C-O_2 surface reaction
out outer region
P carbon dioxide or C-CO_2 surface reaction
s surface
∞ freestream or ambience

Superscripts

j	*j*=0 and 1 designate two-dimensional and axisymmetric flows, respectively
n	reaction order
~	nondimensional or stoichiometrically weighted
′	differentiation with respect to η
*	without water-vapor effect

9. References

Adomeit, G., Hocks, W., & Henriksen, K. (1985). Combustion of a Carbon Surface in a Stagnation Point Flow Field. *Combust. Flame*, Vol. 59, No. 3, pp. 273-288, ISSN 0010-2180.

Adomeit, G., Mohiuddin, G., & Peters, N. (1976). Boundary Layer Combustion of Carbon. *Proc. Combust. Inst.*, Vol. 16, No. 1, pp. 731-743, ISSN 0082-0784.

Annamalai, K. & Ryan, W. (1993). Interactive Processes in Gasification and Combustion-II. Isolated Carbon, Coal and Porous Char Particles. *Prog. Energy Combust. Sci.*, Vol. 19, No. 5, pp. 383-446, ISSN 0360-1285.

Annamalai, K., Ryan, W., & Dhanapalan, S. (1994). Interactive Processes in Gasification and Combustion-Part III: Coal/Char Particle Arrays, Streams and Clouds. *Prog. Energy Combust. Sci.*, Vol. 20, No. 6, pp. 487-618, ISSN 0360-1285.

Arthur, J. R. (1951). Reactions between Carbon and Oxygen. *Trans. Faraday Soc.*, Vol. 47, pp. 164-178.

Batchelder, H. R., Busche, R. M., & Armstrong, W. P. (1953). Kinetics of Coal Gasification. *Ind. Eng. Chem.*, Vol. 45, No. 9, pp. 1856-1878.

Chelliah, H. K., Makino, A., Kato, I., Araki, N., & Law, C. K. (1996). Modeling of Graphite Oxidation in a Stagnation-Point Flow Field Using Detailed Homogeneous and Semiglobal Heterogeneous Mechanisms with Comparisons to Experiments. *Combust Flame*, Vol. 104, No. 4, pp. 469-480, ISSN 0010-2180.

Chung, P. M. (1965). Chemically Reacting Nonequilibrium Boundary Layers. In: *Advances in Heat Transfer*, Vol. 2, J. P. Hartnett, & T. F. Irvine, Jr. (Eds.), Academic, pp. 109-270, ISBN 0-12-020002-3, New York.

Clark, T. J., Woodley, R. E., & De Halas, D. R. (1962). Gas-Graphite Systems, In: *Nuclear Graphite*, R. E. Nightingale (Ed.), pp.387-444, Academic, New York.

Chukhanov, Z. (1938a). The Burning of Carbon. 1. The Sequence of Processes in the Combustion of Air Suspensions of Solid Fuels. *Tech. Phys. USSR.* Vol. 5, pp. 41-58.

Chukhanov, Z. (1938b). The Burning of Carbon. Part II. Oxidation. *Tech. Phys. USSR.* Vol. 5, pp. 511-524.

Eckbreth, A. C. (1988). *Laser Diagnostics for Combustion Temperature and Species*, Abacus, ISBN 2-88449-225-9, Kent.

Essenhigh, R. H. (1976). Combustion and Flame Propagation in Coal Systems: A Review. *Proc. Combust. Inst.*, Vol. 16, No. 1, pp. 353-374, ISSN 0082-0784.

Essenhigh, R. H. (1981). Fundamentals of Coal Combustion, In: *Chemistry of Coal Utilization*, M. A. Elliott (Ed.), pp. 1153-1312, Wiley-Interscience, ISBN 0-471-07726-7, New York.

Gerstein, M. & Coffin, K. P. (1956). Combustion of Solid Fuels, In: *Combustion Processes*, B. Lewis, R. N. Pease, and H. S. Taylor (Eds.), Princeton UP, Princeton, pp.444-469.

Harris, D. J. & Smith, I. W. (1990), Intrinsic Reactivity of Petroleum Coke and Brown Coal Char to Carbon Dioxide, Steam and Oxygen. *Proc. Combust. Inst.*, Vol. 23, No. 1, pp. 1185-1190, ISSN 0082-0784.

Henriksen, K. (1989). Weak Homogeneous Burning in Front of a Carbon Surface. *Proc. Combust. Inst.*, Vol. 22, No. 1, pp. 47-57, ISSN 0082-0784.

Henriksen, K., Hocks, W., & Adomeit, G. (1988). Combustion of a Carbon Surface in a Stagnation Point Flow Field. Part II: Ignition and Quench Phenomena. *Combust. Flame*, Vol. 71, No. 2, pp. 169-177, ISSN 0010-2180.

Howard, J. B., Williams, G. C., & Fine, D. H. (1973). Kinetics of Carbon Monoxide Oxidation in Postflame Gases. *Proc. Combust. Inst.*, Vol. 14, No. 1, pp. 975-986, ISSN 0082-0784.

Khitrin, L. N. (1962). *The Physics of Combustion and Explosion*, Israel Program for Scientific Translations, Jerusalem.

Khitrin, L. N. & Golovina, E. S. (1964). Interaction between Graphite and Various Chemically Active Gases at High Temperatures. In: *High Temperature Technology*, Butterworths, London, pp. 485-496.

Kurylko, L. and Essenhigh, R. H. (1973). Steady and Unsteady Combustion of Carbon. *Proc. Combust. Inst.*, Vol. 14, No. 1, pp. 1375-1386, ISSN 0082-0784.

Law, C. K. (1978). On the Stagnation-Point Ignition of a Premixed Combustion. *Int. J. Heat Mass Transf.*, Vol. 21, No. 11, pp. 1363-1368, ISSN 0017-9310.

Libby, P. A. & Blake, T. R. (1979). Theoretical Study of Burning Carbon Particles. *Combust. Flame*, Vol. 36, No. 1, pp. 139-169, ISSN 0010-2180.

Liñán, A. (1974). The Asymptotic Structure of Counter Flow Diffusion Flames for Large Activation Energies. *Acta Astronautica*, Vol. 1, No. 7-8, pp. 1007-1039, ISSN 0094-5765.

Maahs, H. G. (1971). Oxidation of Carbon at High Temperatures: Reaction-Rate Control or Transport Control. NASA TN D-6310.

Makino, A. (1990). A Theoretical and Experimental Study of Carbon Combustion in Stagnation Flow. *Combust. Flame*, Vol. 81, No. 2, pp. 166-187, ISSN 0010-2180.

Makino, A. (1992). An Approximate Explicit Expression for the Combustion Rate of a small Carbon Particle. *Combust. Flame*, Vol. 90, No. 2, pp. 143-154, ISSN 0010-2180.

Makino, A. & Law, C. K. (1986). Quasi-steady and Transient Combustion of a Carbon Particle: Theory and Experimental Comparisons. *Proc. Combust. Inst.*, Vol. 21, No. 1, pp. 183-191, ISSN 0082-0784.

Makino, A. & Law, C. K. (1990). Ignition and Extinction of CO Flame over a Carbon Rod. *Combust. Sci. Technol.*, Vol. 73, No. 4-6, pp. 589-615, ISSN 0010-2202.

Makino, A., Araki, N., & Mihara, Y. (1994). Combustion of Artificial Graphite in Stagnation Flow: Estimation of Global Kinetic Parameters from Experimental Results. *Combust. Flame*, Vol. 96, No. 3, pp. 261-274, ISSN 0010-2180.

Makino, A., Kato, I., Senba, M., Fujizaki, H., & Araki, N. (1996). Flame Structure and Combustion Rate of Burning Graphite in the Stagnation Flow. *Proc. Combust. Inst.*, Vol. 26, No. 2, pp. 3067-3074, ISSN 0082-0784.

Makino, A., Namikiri, T., & Araki, N. (1998). Combustion Rate of Graphite in a High Stagnation Flowfield and Its Expression as a Function of the Transfer Number. *Proc. Combust. Inst.*, Vol. 27, No. 2, pp. 2949-2956, ISSN 0082-0784.

Makino, A., Senba, M., Shintomi, M., Fujizaki, H., & Araki, N. (1997). Experimental Determination of the Spatial Resolution of CARS in the Combustion Field – CARS Thermometry Applied to the Combustion Field of Solid Carbon in a Stagnation Flow – . *Combust. Sci. Technol., Jpn*., Vol. 5, No. 2, pp. 89-101, ISSN 0918-5712. [in Japanese].

Matalon, M. (1980). Complete Burning and Extinction of a Carbon Particle in an Oxidizing Atmosphere. *Combust. Sci. Technol.*, Vol. 24, No. 3-4, pp. 115-127, ISSN 0010-2202.

Matalon, M. (1981). Weak Burning and Gas-Phase Ignition about a Carbon Particle in an Oxidizing Atmosphere. *Combust. Sci. Technol.*, Vol. 25, No. 1-2, pp. 43-48, ISSN 0010-2202.

Matalon, M. (1982). The Steady Burning of a Solid Particle. SIAM J. Appl. Math., Vol. 42, No. 4, pp. 787-803, ISSN 0036-1399.

Matsui, K., Kôyama, A., & Uehara, K. (1975). Fluid-Mechanical Effects on the Combustion Rate of Solid Carbon. *Combust. Flame*, Vol. 25, No. 1, pp. 57-66, ISSN 0010-2180.

Matsui, K. & Tsuji, H. (1987). An Aerothermochemical Analysis of Solid Carbon Combustion in the Stagnation Flow Accompanied by Homogeneous CO Oxidation. *Combust. Flame*, Vol. 70, No. 1, pp. 79-99, ISSN 0010-2180.

Matsui, K., Tsuji, H., & Makino, A. (1983). The Effects of Water Vapor Concentration on the Rate of Combustion of an Artificial Graphite in Humid Air Flow. *Combust. Flame*, Vol. 50, No. 1, pp. 107-118, ISSN 0010-2180.

Matsui, K., Tsuji, H., & Makino, A. (1986). A Further Study of the Effects of Water Vapor Concentration on the Rate of Combustion of an Artificial Graphite in Humid Air Flow. *Combust. Flame*, Vol. 63, No. 3, pp. 415-427, ISSN 0010-2180.

Mulcahy, M. F. & Smith, I. W. (1969). Kinetics of Combustion of Pulverized Fuel: A Review of Theory and Experiment. *Rev. Pure and Appl. Chem.*, Vol. 19, No. 1, pp. 81-108.

Nagel, J. & Strickland-Constable, R. F. (1962). Oxidation of Carbon between 1000-2000°C. *Proc. Fifth Conf. On Carbon*, pp. 154-164, Pergamon, New York.

Rosner, D. E. (1972). High-Temperature Gas-Solid Reactions, *Annual Review of Materials Science*, Vol. 2, pp. 573-606, ISSN 0084-6600.

Sobolev, G. K., (1959). High-Temperature Oxidation and Burning of Carbon Monoxide. *Proc. Combust. Inst.*, Vol. 7, No. 1, pp. 386-391, ISSN 0082-0784.

Spalding, D. B. (1951). Combustion of Fuel Particles. *Fuel*, Vol. 30, No. 1, pp. 121-130, ISSN 0016-2361

Tsuji, H. & Matsui, K. (1976). An Aerothermochemical Analysis of Combustion of Carbon in the Stagnation Flow. *Combust. Flame*, Vol. 26, No. 1, pp. 283-297, ISSN 0010-2180.

Tsuji, H. & Yamaoka, I. (1967). The Counterflow Diffusion Flame in the Forward Stagnation Region of a Porous Cylinder. *Proc. Combust. Inst.*, Vol. 11, No. 1, pp. 979-984. ISSN 0082-0784.

Visser, W. & Adomeit, G. (1984). Experimental Investigation of the Ignition and Combustion of a Graphite Probe in Cross Flow. *Proc. Combust. Inst.*, Vol. 20, No. 2, pp. 1845-1851, ISSN 0082-0784.

Walker, P. L., Jr., Rusinko, F., Jr., & Austin, L. G. (1959). Gas Reaction of Carbon, In: *Advances in Catalysis and Related Subjects*, Vol. 11, D. D. Eley, P. W. Selwood, & P. B. Weisz (Eds.), pp. 133-221, Academic, ISBN 0-12-007811-2, New York.

Yang, R. T. & Steinberg, M. (1977). A Diffusion Cell Method for Studying Heterogeneous Kinetics in the Chemical Reaction/Diffusion Controlled Region. Kinetics of C + CO_2→ 2CO at 1200-1600°C. *Ind. Eng. Chem. Fundam.*, Vol. 16, No. 2, pp. 235-242, ISSN 0196-4313.

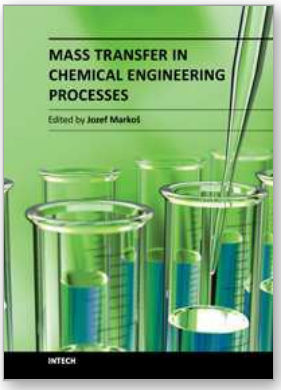

Mass Transfer in Chemical Engineering Processes

Edited by Dr. Jozef MarkoÅ¡

ISBN 978-953-307-619-5
Hard cover, 306 pages
Publisher InTech
Published online 04, November, 2011
Published in print edition November, 2011

This book offers several solutions or approaches in solving mass transfer problems for different practical chemical engineering applications: measurements of the diffusion coefficients, estimation of the mass transfer coefficients, mass transfer limitation in separation processes like drying, extractions, absorption, membrane processes, mass transfer in the microbial fuel cell design, and problems of the mass transfer coupled with the heterogeneous combustion. I believe this book can provide its readers with interesting ideas and inspirations or direct solutions of their particular problems.

How to reference

In order to correctly reference this scholarly work, feel free to copy and paste the following:

Atsushi Makino (2011). Mass Transfer Related to Heterogeneous Combustion of Solid Carbon in the Forward Stagnation Region - Part 1 - Combustion Rate and Flame Structure, Mass Transfer in Chemical Engineering Processes, Dr. Jozef MarkoÅ¡ (Ed.), ISBN: 978-953-307-619-5, InTech, Available from: http://www.intechopen.com/books/mass-transfer-in-chemical-engineering-processes/mass-transfer-related-to-heterogeneous-combustion-of-solid-carbon-in-the-forward-stagnation-region-1

INTECH
open science | open minds

InTech Europe
University Campus STeP Ri
Slavka Krautzeka 83/A
51000 Rijeka, Croatia
Phone: +385 (51) 770 447
Fax: +385 (51) 686 166
www.intechopen.com

InTech China
Unit 405, Office Block, Hotel Equatorial Shanghai
No.65, Yan An Road (West), Shanghai, 200040, China
中国上海市延安西路65号上海国际贵都大饭店办公楼405单元
Phone: +86-21-62489820
Fax: +86-21-62489821